

We are IntechOpen, the world's leading publisher of Open Access books Built by scientists, for scientists

6,900

Open access books available

186,000

International authors and editors

200M

Downloads

Our authors are among the

154

Countries delivered to

TOP 1%

most cited scientists

12.2%

Contributors from top 500 universities



WEB OF SCIENCE™

Selection of our books indexed in the Book Citation Index
in Web of Science™ Core Collection (BKCI)

Interested in publishing with us?
Contact book.department@intechopen.com

Numbers displayed above are based on latest data collected.
For more information visit www.intechopen.com



Combined Transmission Electron Microscopy – *In situ* Observation of the Formation Process and Measurement of Physical Properties for Single Atomic-Sized Metallic Wires

Hideki Masuda

Additional information is available at the end of the chapter

<http://dx.doi.org/10.5772/62288>

Abstract

This chapter introduces the research of *in situ* high-resolution transmission electron microscope (HRTEM) methods combined with the functions of atomic force microscope and scanning tunneling microscope. Using this method, we demonstrate fabrication, dynamic observation on an atomistic scale, and mechanical and electrical measurements of nanometer-sized contact simultaneously. We evaluate the silver atomic-sized wire (ASW) which appeared at the final stage of the rupture process of the silver nano-contact.

Keywords: Silver, atomic-sized wires, atomic force microscopy, high-resolution transmission electron microscopy

1. Introduction

Currently, miniaturization of electronics is underway. Now device development is heading toward atomistic and molecular scales [1]. Devices included in these circuits are nanometer-sized contacts (NCs), atomic-sized wires (ASWs), single molecular junctions (SMJs), etc. (Figure 1) [2]. SMJ is a system of single molecule sandwiched by a pair of nanometer-sized metallic electrodes. SMJs enable single electronic operation, high-density integration, and electric power saving [3-7]. To engineer SMJs, we need to reveal that the structure of device configuration includes interfaces between molecules and electrodes and mechanical and electrical properties. Metallic NCs and ASWs are fundamental materials that have the potential for device applications as well as being the key factors required for the application of SMJs [8].

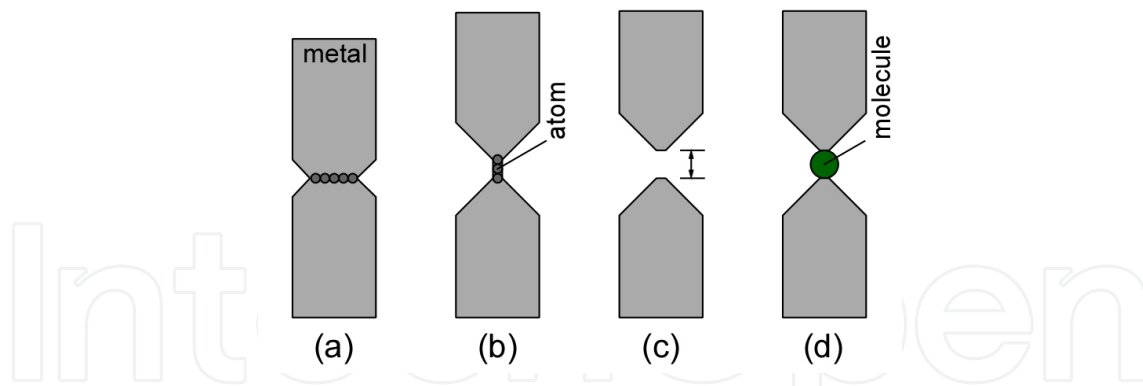


Figure 1. Schematics of atomistic-scale devices. (a) NC; (b) ASW; (c) nano-gap structure; and (d) SMJ.

Actually, to observe the formation and deformation of NCs, two *in situ* high-resolution transmission electron microscope (HRTEM) methods were developed; one is the electron beam double holes drilling method. An electron beam drills two holes on a material film with a focused beam. The bridge that was formed between the holes is gradually deformed using a defocused electron beam [9]. The other method is the tip-sample contact method [10], and this fabricates and deforms NCs using a piezo-driven tip. Kizuka and Tanaka observed Zn NCs using this method in HRTEM in 1994 [11]. In 1998, Kizuka et al. directly observed the slip deformation process of Au NCs (Figure 2) [12]. This is the first report that showed atomistic-level observation of a slip deformation process in crystals. After that, Ohnishi et al. fabricated Au NCs and observed the deformation process from a 5-atom width to an 1-atom width in 1998 [13].

In 2001, Kizuka et al. observed the deformation process of Au NCs with atomistic resolution using HRTEM based on the *in situ* method combined with atomic force microscope (AFM) and scanning tunneling microscope (STM) [10]. They measured stress and strain quantitatively and started material mechanics research of metallic NCs. Using this method, the mechanical properties of Cu [14], Ir [15], Pd [16], and Pt [17] NCs were researched.

Further, as Kizuka et al. improved the *in situ* HRTEM method [18]; they were able to observe the structural dynamics of ASWs formation during the tensile deformation process and research electrical and mechanical properties. Using this method, it was revealed that there was a corresponding relationship between structural dynamics and physical properties [19]. Until that point in time they had been researched individually. They observed Au ASW at the final stage of the tensile deformation process of Au NCs. The observed Au ASW is up to 10 atoms in length with an average interatomic distance of 0.27 nm (Figure 3). In the tensile deformation process of ASWs, since tensile stress is concentrated on the contact region, interatomic distances of Au ASWs become longer, up to 0.30 nm. At the same time, conductance of Au ASWs was measured. Resultant conductance greatly decreases when the number of atoms used to construct the ASWs exceeds 4. Moreover, the force acting on the contact was measured. The tensile strength of this ASW was estimated to be from 8 to 17 GPa. This value is several times larger than that of Au NCs and much larger than bulk Au.

At elastic deformation regions undergoing stress–strain, the Young’s modulus of Au ASWs was estimated to be between 47 and 116 GPa. This value is remarkably comparable with that of a single crystal Au.

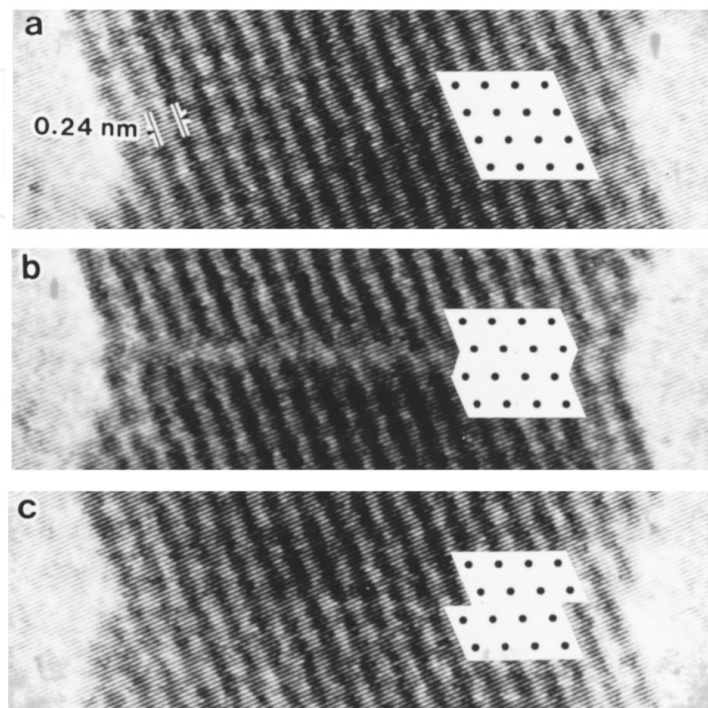


Figure 2. Time variation in the elementary steps of slip in the shear deformation of Au NCs [12].

The NCs and ASWs of other materials other than Au have been also observed. Au, Ag [20, 21], Cu [22], Pt [17, 23], Pd [23, 24], Ir [15], and Co [23] ASWs have been observed.

As described above, common problems in research in metallic ASWs and NCs existed, revealing corresponding relationships between structure and electrical properties. As research in ASWs has concentrated on Au, the structural dynamics of ASW formation is uncertain. For some of the metallic ASWs already researched, only the structures that appeared in the tensile deformation process of NCs were observed. Therefore, the stable structure and electrical conductivity of the NCs have not yet been revealed. In order to produce a general rule for the basic phenomenon that appears in metallic NCs and ASWs, it is necessary to examine structural dynamics, electrical conductivity, and mechanical properties, in order to clarify the corresponding relationship between the structure and properties directly. The method is limited to *in situ* HRTEM.

2. Combined HRTEM

For the *in situ* tip-sample contact experiment inside the HRTEM, we proposed inserting multiple specimen holders in the specimen chamber. The secondary holder is usually intro-

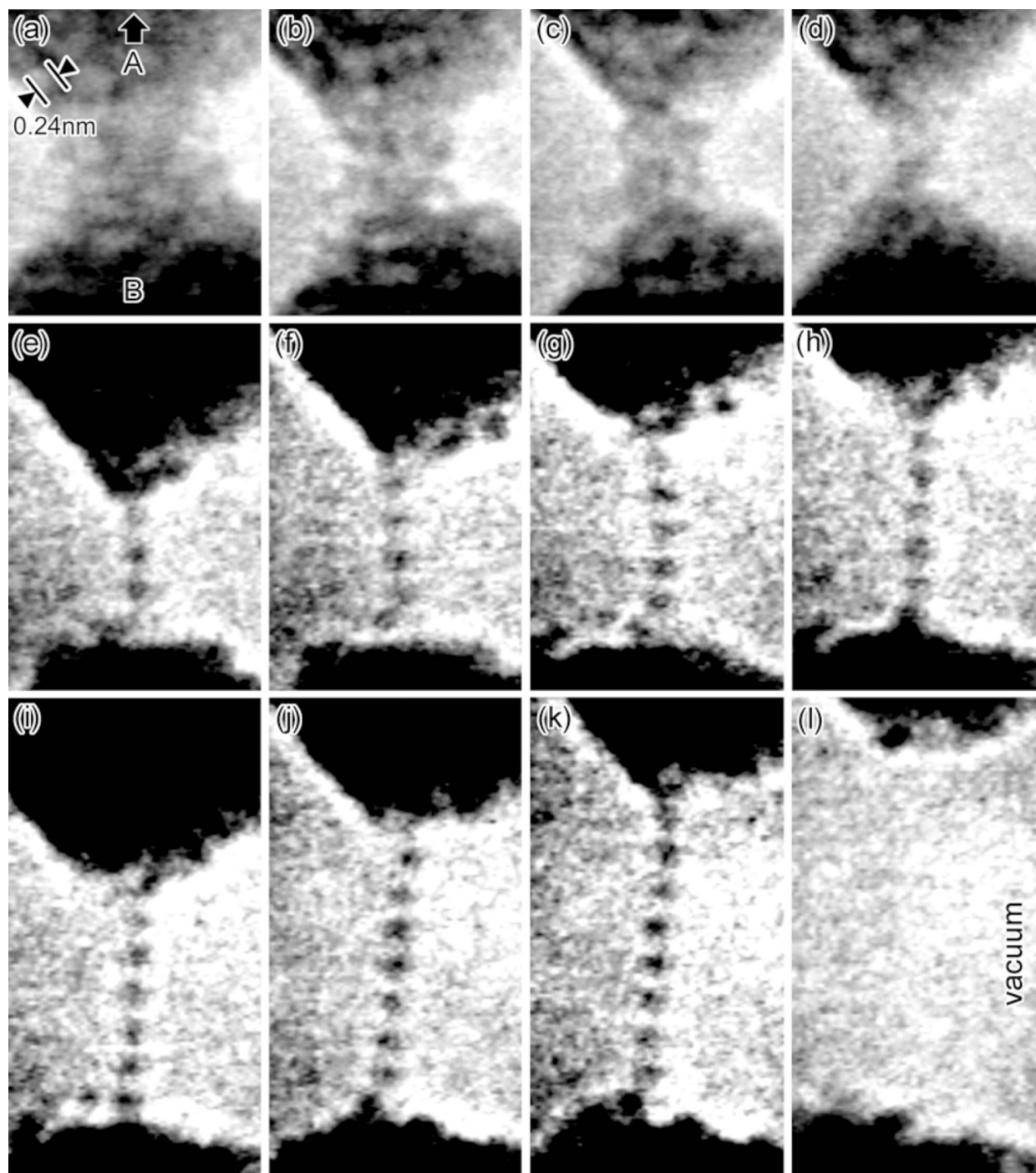


Figure 3. Time variation of the Au ASW formation process observed using the *in situ* HRTEM method [19].

duced from the direction perpendicular to the first holder (Figure 4). Since this space is often used for an EDX detector, it is necessary to replace it. In addition, we should consider that this is a space occupying in *z* direction; the relation between the gap distance of pole pieces and the height of sample holders (Figure 5). When you want to do mechanical tests, for example, you would introduce an AFM cantilever. In this configuration, it is rarely applied to a pole piece for high resolution use. This is because the samples must be precisely adjusted to contact

at the standard focal position of the microscope, including the movement range in the z direction of the goniometer, which is attached to each holder.

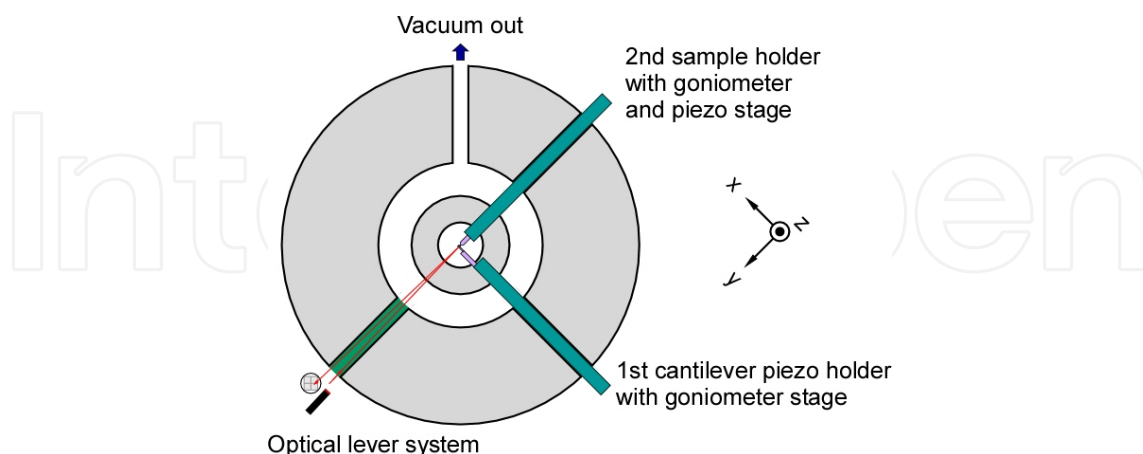


Figure 4. Illustration depicting the specimen chamber of the HRTEM combined with atomic force microscope (AFM).

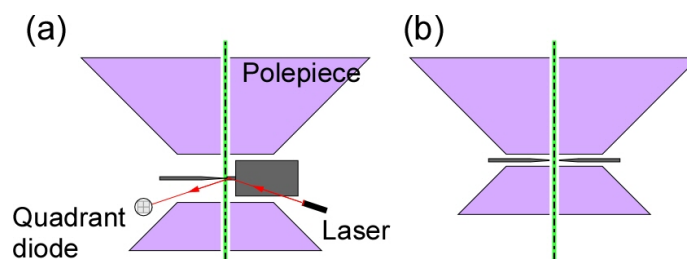


Figure 5. Illustrations depicting the configuration of samples and pole pieces for a combined HRTEM.

3. Sample preparation

For samples, we use a cut-out metal foil and the metal sputtered tip of the AFM cantilever. In the case of metallic foil, first we cut out the foil with a thickness of below 0.05 mm to a size of 1 mm by 10 mm and sharpen one side of the plate (Figure 6(a)). After that, we polish this side mechanically using emery papers and aluminum or diamond wrapping film. In rare cases, although a burr part of cut is sometimes thin enough for HRTEM observation, the yield is poor and the workability of nano-tip creation processes in a HRTEM is not good because the sample is affected by a stress concentration where there is a sudden change in thickness. This sample is then thinned further by an Ar ion polish of 3–10 kV (Figure 6(b)). It may be that an ionic cleaner is used just before introducing it into a vacuum.

When performing the mechanical tests simultaneously, it is suggested that you use a metallic sputtered Si tip on the cantilever for AFM for one of the samples (Figure 7). For high-resolution (HR) observations, in order to detect the small force needed to deform the fine structure, the

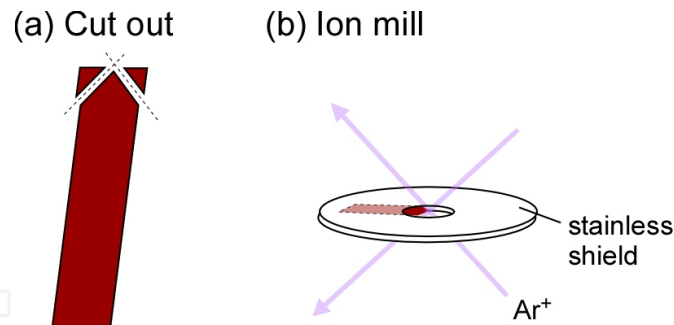


Figure 6. Illustrations showing the downsize process of metal foil.

spring constant of the cantilever is required to be small (5 N/m or less is preferred). Metal is sputtered on the cantilever and the tip under a reduced pressure Ar atmosphere. The thickness of metallic film is approximately 20 nm. The requirements in this process are (i) depositing metal atoms on the tip for use in contact with the counter sample and (ii) ensuring the cantilever surface is covered with a uniform continuous metallic film to offer sufficient conductivity. In order to achieve the latter requirement, it would be preferable to sputter in the same way on both sides of cantilever. Moreover, even if the required amount of sputtering is achieved, the spring constant of the cantilever is not changed.

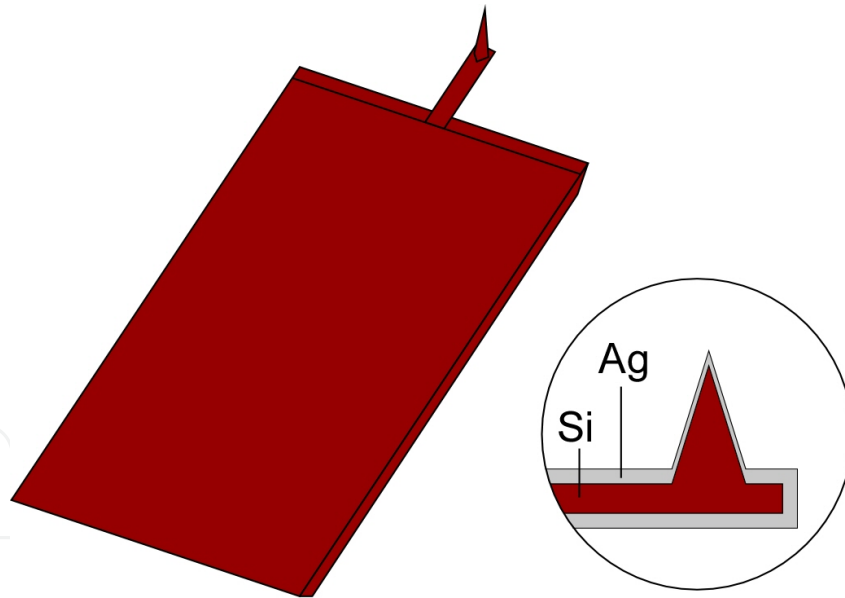


Figure 7. Illustration of cantilever preparation for the Ag contact experiment.

Both samples are attached to a specimen holder respectively, then inserted into the HRTEM specimen chambers. Because the sample is exposed to air for several minutes during this preparation process, a natural oxide or sulfide film is deposited on the sample surface. After the first contact with the sample each other, once we should make the contact larger than a width of several tens nanometers. This is because we pull a clean metal part to the surface from inside the samples.

4. Observation of Ag ASWs

Figure 8 shows HR images during the process of miniaturization of Ag NCs. The black areas at the top and bottom of each image are Ag, the center is the NC, and the surrounding area is a vacuum. On all of the NCs, a lattice interval of Ag (0.24 nm) has appeared – as indicated by (111) in the figure. That is, the contact region is a single crystal. Therefore, the direction of incidence of the electron beam is indicated on the figure as [0-11] and the upward direction on image is identified as [100] in the figure. The minimum cross-sectional width of the NC is (a) 4 atoms, (b) 3 atoms, and (c–e) 1 atom. Figure 8(f) shows the contact braking.

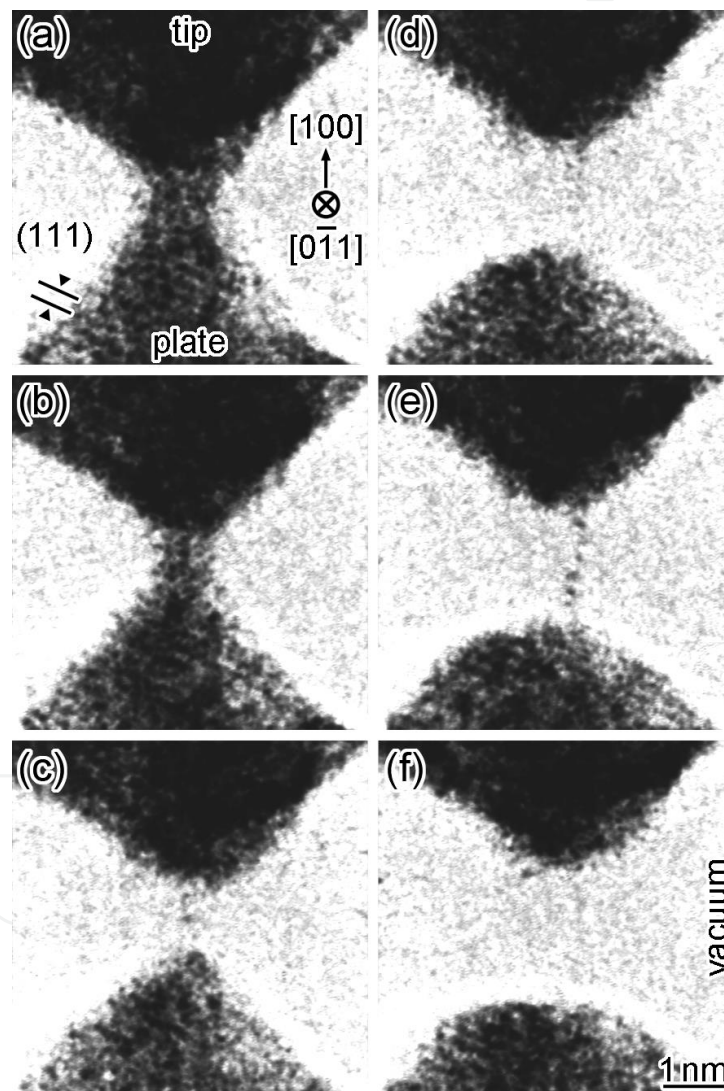


Figure 8. Time variation of Ag ASW formation process observed by *in situ* HRTEM.

Figure 9, it shows the calculated image and HR image for the Ag ASW. For the image calculation, we used a model in which both ends of the wire (composed of seven atoms) were connected to two pyramidal Ag crystals (Figure 9(a)). Seven of the Ag ASW atoms were along

the [100] crystal pyramid and arranged at intervals of 0.289 nm, which is the nearest neighboring distance of the bulk Ag. Figure 9(b) is a calculated image for the model. In Figure 9(c), the image intensity along the center line of the atomic wires is shown. The centers of the models of the atoms are displaced from the centers of the black point in computational image by only 0–0.02 nm. Since the experimental spatial resolution of the current HRTEM observation is 0.1 nm, the calculated result agree with the experimentally observed image within that resolution. This correspondence is similar to that of Au atoms in a wire [19]. Figure 9(d) is an enlarged view of the Ag ASW shown in Figure 8(e). Figure 9(c and e) shows the image intensity along the center line of the ASWs. The darkest positions are indicated by the arrows. From the results of the image calculation, the atomic positions of the ASWs can be considered to correspond to the darkest position in the image intensity.

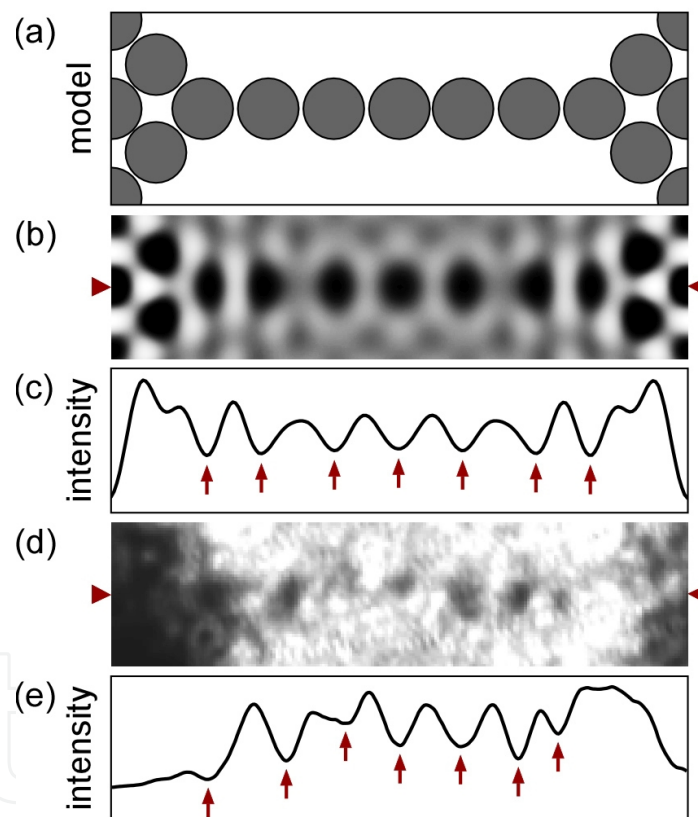


Figure 9. HR images of Ag ASWs. (a) Projected model along [110]; (b) calculated image for the structural model of (a); (c) line profile of (b); (d) enlarged experimental image of Figure 8(e); and (e) line profile of (d).

Figure 10 shows the time variation of force and conductance in the Ag ASW formation process shown in Figure 8. Times (a–f) correspond to the times that each image in Figure 8 was observed, respectively. As the NC narrowed, the conductance stepwise reduced (a–b). Similarly, the force acting on the NC also decreased stepwise. Thereafter, when the ASW forms (c–e), both conductance and force were reduced below $0.1 G_0$ and 0.5 nN.

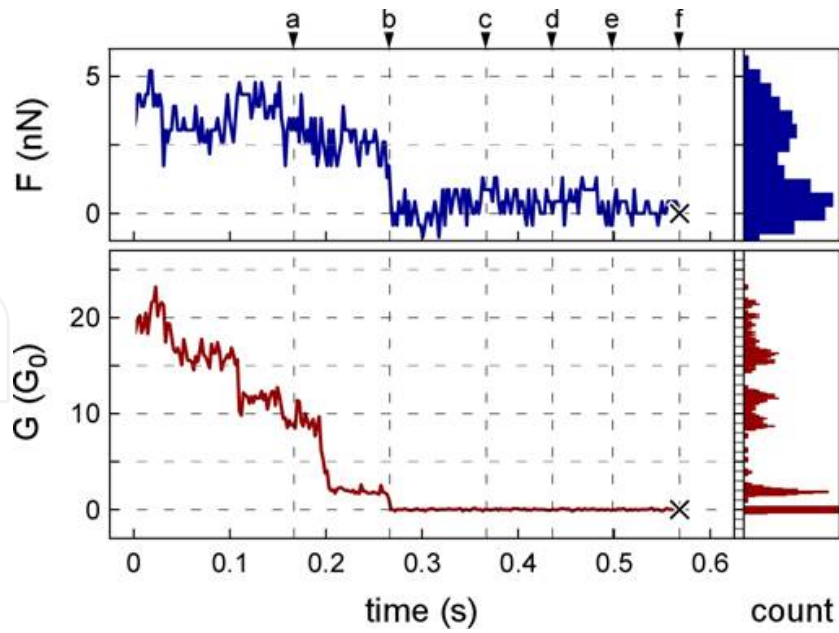


Figure 10. Time variation in the force and conductance measured in the deformation process of Figure 8.

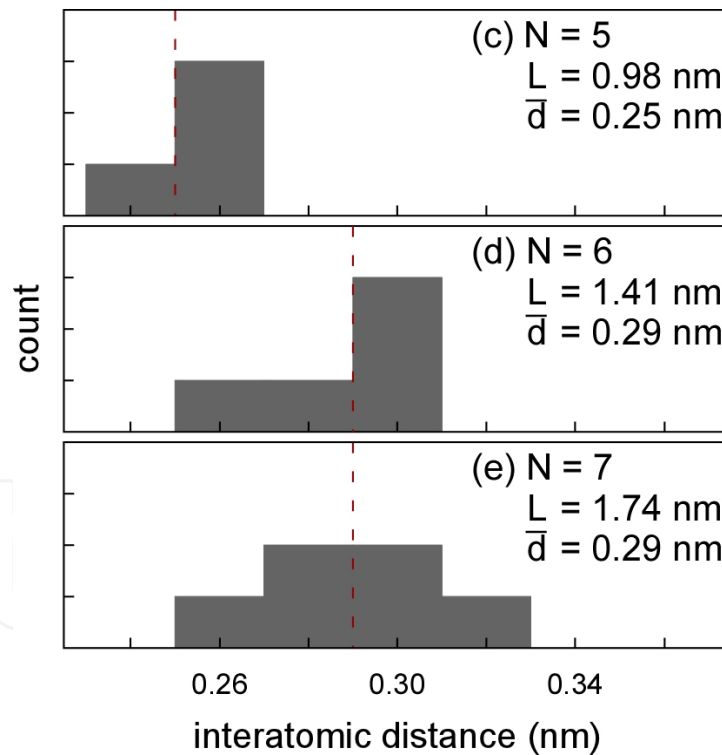


Figure 11. Distribution of interatomic distances in Ag ASWs.

Figure 11 shows the distribution of the interatomic distances between atoms in the wire, observed in Figure 8. When the number of atoms in the ASW was five, the interatomic distance was 0.25 ± 0.01 nm. However, this became 0.29 ± 0.05 nm for an ASW comprised of six or seven atoms. In other words, as the ASW becomes longer, the interatomic distance increases.

ASWs are generally considered to be formed by pulling out atoms one by one from the electrode. Bahn and Jacobsen calculated the process of pulling metal NCs (Figure 12) using the density functional method via molecular dynamics calculations and effective medium approximation [25]. In the state where tip atoms, from two pyramid-shaped electrodes, bond to one another, the single atom located at the minimum cross-section part bonds to not only three or four atoms of the electrode side but also atoms at the opposite electrode simultaneously. They estimated the bonding strength between these atoms, then went on to discuss whether this monatomic junction can draw atoms from the electrode without leading to a fracture. As a result, for Au and Pt, the strength of the binding of atoms in the wire part is energetically three times larger than that in the electrode part; it tends to form ASWs. On the other hand, for Cu, Ag, Ni, and Pd, it is difficult to form ASWs in this way.

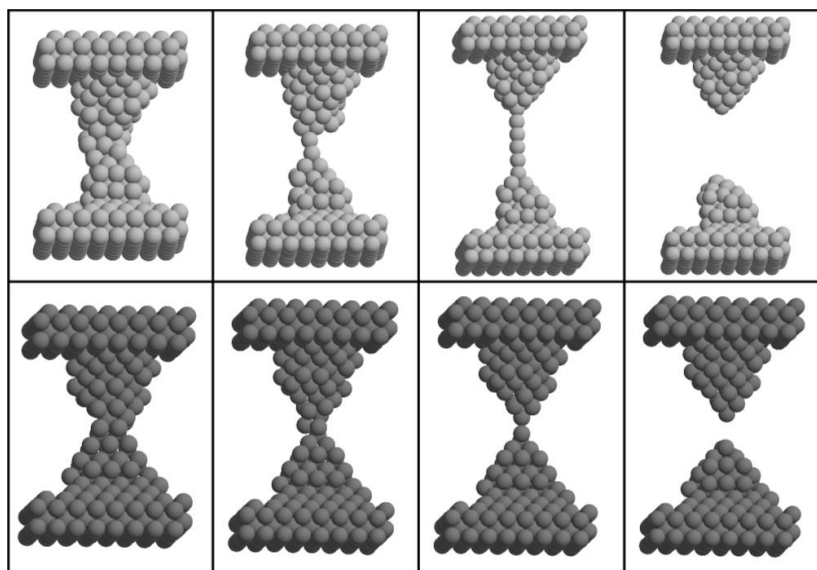


Figure 12. MD simulation of the tensile deformation process for Au (upper) and Cu (lower) NCs [25].

In the experiment shown in Figure 8, Ag ASWs were formed by tensile deformation of NCs. Since as soon as the NC is miniaturized to one atom width (Figure 8(b)), it forms four or more atomic length wires, the stretching process from a single atom contact could not be observed. In other words, the structural change from the Ag NC to the Ag ASW was faster than the frame rate available using TEM observations (~ 17 ms). Moreover, we have applied a voltage of 13 mV for the conductance measurement. The withdrawal of atoms from the electrode for atomic wires involved not only tensile force, but also atom transfer by electron wind force. As an example of this effect, when we apply a voltage of 100 mV to the NC, ASW with a length of ~ 0.88 nm formed just before breaking without applying tensile force [8]. Therefore, even for some of the elements for which ASWs were hardly expected to form, there remains the possibility of wire formation due to the atomic diffusion effect.

5. Conclusion

In this chapter, we introduced combined microscopy techniques which are based on HRTEM, AFM, and STM. This approach was developed to meet the demand for characterization of nanostructures which needs correspondence between the structure and the physical properties directly. In fact, this research has been promoted with respect to the junction between nano-scales or atomistic scales for a single metal. In the future, this method needs to be combined with chemical reaction engineering for single molecular device fabrication, such as catalysts, corrosion, and storage devices.

Acknowledgements

This work was partly supported by Grant-in-Aid for JSPS Fellows (10J01479).

Author details

Hideki Masuda*

Address all correspondence to: masuda.hideki@nims.go.jp

National Institute for Materials Science, Tsukuba, Japan

References

- [1] Cuevas, JC, and Scheer, E, *Molecular Electronics: An Introduction to Theory and Experiment*. World Scientific, Singapore, 2010.
- [2] Joachim, C, Gimzewski, JK, and Aviram, A: Electronics using hybrid-molecular and mono-molecular devices. 2000; 408: 541. *Nature*.
- [3] Di Ventra, M, Pantelides, ST, and Lang, ND: First-principles calculation of transport properties of a molecular device. 2000; 84: 979. *Physical Review Letters*.
- [4] Kubatkin, S *et al.*: Single-electron transistor of a single organic molecule with access to several redox states. 2003; 425: 698. *Nature*.
- [5] Tao, NJ: Electron transport in molecular junctions. 2006; 1: 173. *Nature Nanotechnology*.

- [6] Danilov, A *et al.*: Electronic transport in single molecule junctions: Control of the molecule-electrode coupling through intramolecular tunneling barriers. 2007; 8: 1. Nano Letters.
- [7] Kim, WY, *et al.*: Application of quantum chemistry to nanotechnology: Electron and spin transport in molecular devices. 2009; 38: 2319. Chemical Society Reviews.
- [8] Masuda, H, and Kizuka, T: Distance control of electromigration-induced silver nanogaps. 2014; 14: 2436. Journal of Nanoscience and Nanotechnology.
- [9] Kondo, Y, and Takayanagi, K: Gold nanobridge stabilized by surface structure. 1997; 79: 3455. Physical Review Letters.
- [10] Kizuka, T, *et al.*: Simultaneous observation of millisecond dynamics in atomistic structure, force and conductance on the basis of transmission electron microscopy. 2001; 40: L170. Japanese Journal of Applied Physics.
- [11] Kizuka, T, and Tanaka, N: Dynamic high-resolution electron microscopy of diffusion bonding between zinc oxide nanocrystallites at ambient temperature. 1994; 69: 135. Philosophical Magazine Letters.
- [12] Kizuka, T: Atomistic visualization of deformation in gold. 1998; 57: 11158. Physical Review B.
- [13] Ohnishi, H, Kondo, Y, and Takayanagi, K: Quantized conductance through individual rows of suspended gold atoms. 1998; 395: 780. Nature.
- [14] Fujisawa, S, Kikkawa, T, and Kizuka, T: Direct observation of electromigration and induced stress in Cu nanowire. 2003; 42: L1433. Japanese Journal of Applied Physics.
- [15] Ryu, M, and Kizuka, T: Structure, conductance and strength of iridium wires of single atom width. 2006; 45: 8952. Japanese Journal of Applied Physics.
- [16] Matsuda, T, and Kizuka, T: Structure of nanometer-sized palladium contacts and their mechanical and electrical properties. 2007; 46: 4370. Japanese Journal of Applied Physics.
- [17] Kizuka, T, and Monna, K: Atomic configuration, conductance, and tensile force of platinum wires of single-atom width. 2009; 80: 205406. Physical Review B.
- [18] Kizuka, T, Umehara, S, and Fujisawa, S: Metal-insulator transition in stable one-dimensional arrangements of single gold atoms. 2001; 40: L71. Japanese Journal of Applied Physics.
- [19] Kizuka, T: Atomic configuration and mechanical and electrical properties of stable gold wires of single-atom width. 2008; 77: 155401. Physical Review B.
- [20] Rodrigues, V *et al.*: Quantum conductance in silver nanowires: Correlation between atomic structure and transport properties. 2002; 65: 153402. Physical Review B.

- [21] Lagos, MJ, *et al.*: Observation of the smallest metal nanotube with a square cross-section. 2009; 4: 149. *Nature Nanotechnology*.
- [22] González, JC, *et al.*: Indication of unusual pentagonal structures in atomic-size Cu nanowires. 2004; 93: 126103. *Physical Review Letters*.
- [23] Rodrigues, V, *et al.*: Evidence for spontaneous spin-polarized transport in magnetic nanowires. 2003; 91: 096801. *Physical Review Letters*.
- [24] Matsuda, T, and Kizuka, T: Palladium wires of single atom width as mechanically controlled switching devices. 2006; 45: L1337. *Japanese Journal of Applied Physics*.
- [25] Bahn, SR, and Jacobsen, KW: Chain formation of metal atoms. 2001; 87: 266101. *Physical Review Letters*.

IntechOpen

